VOLUME 115, NUMBER 19
SEPTEMBER 22, 1993

JOURNAL
OF THE
AMERICAN
CHEMICAL
SOCIETY

Phospholipase A_2 Engineering. 10. The Aspartate···Histidine Catalytic Diad Also Plays an Important Structural Role[1]

Yishan Li[†] and Ming-Daw Tsai[*]

Contribution from the Departments of Chemistry and Biochemistry and The Ohio State Biochemistry Program, The Ohio State University, Columbus, Ohio 43210

Received April 8, 1993[⊗]

Abstract: The "catalytic triad" of serine proteases and lipases and the "catalytic diad" of phospholipase A_2 (PLA2) are the key catalytic machineries of these enzymes. We present evidence that the catalytic diad of PLA2 also plays an important structural role. The His-48 of PLA2 was changed to Asn, Gln, and Ala; the resulting mutants are named H48N, H48Q, and H48A, respectively. The amide nitrogen atoms of Asn and Gln mimic the δ_1-nitrogen and the ϵ_2-nitrogen, respectively, of His. According to the crystal structure, the δ_1-nitrogen is the actual general base while the ϵ_2-nitrogen is hydrogen-bonded to Asp-99. Kinetic analysis indicated that H48N retains 6×10^{-5} of original activity while H48Q and H48A show no detectable activity. On the other hand, proton NMR and conformational stability analyses indicated that the conformation of the enzyme is largely retained in H48Q but is highly perturbed in H48N and H48A. The results suggest that while the δ_1-nitrogen of His-48 is important for the catalysis by PLA2, the ϵ_2-nitrogen of the same residue plays an important structural role.

Introduction

The Asp···His···Ser "catalytic triad" is the key catalytic machinery of serine proteases and, as discovered recently, lipases[2] as well. Phospholipase A_2 (PLA2)[1] uses a similar machinery involving the Asp-99···His-48 "catalytic diad".[3] The function of serine is replaced by a water molecule hydrogen-bonded to the δ_1-nitrogen of His-48, as shown in Figure 1.[4] The catalytic functions of the triad and the diad residues have been studied extensively throughout the history of biochemistry, including the use of site-directed mutagenesis in recent years.[5] However, to our knowledge, there has never been a suggestion that these residues also play structural roles other than holding one another in place. In this study, we employed site-directed mutagenesis in combination with structural analyses using both proton NMR and conformational stability to explore the detailed roles of the imidazole ring of His-48 in PLA2. Our system is bovine pancreatic PLA2 overexpressed in *Escherichia coli*.[6] The results suggest

† The Ohio State Biochemistry Program.
* Departments of Chemistry and Biochemistry and The Ohio State Biochemistry Program. Address correspondence to this author at the Department of Chemistry, 120 West 18th Avenue, Columbus, Ohio 43210.
⊗ Abstract published in *Advance ACS Abstracts*, September 1, 1993.

(1) For paper 9 in this series, see ref 7b. Abbreviations: 1D, one-dimensional; 2D, two-dimensional; CD, circular dichroism; DC_8PC, 1,2-dioctanoyl-*sn*-3-phosphocholine; DQF-COSY, double quantum filtered correlated spectroscopy; FPLC, fast protein liquid chromatography; Gdn–HCl, guanidine hydrochloride; NMR, nuclear magnetic resonance; NOE, nuclear Overhauser effect; NOESY, nuclear Overhauser enhancement spectroscopy; PAGE, polyacrylamide gel electrophoresis; PLA2, phospholipase A_2; SDS, sodium dodecyl sulfate; TMSP, sodium 3-(trimethylsilyl)propionate-*2,2,3,3-d*$_4$; and WT, wild type.

(2) (a) Brady, L.; Brzozowski, A. M.; Derewenda, Z. S.; Dodson, E.; Dodson, G.; Tolley, S.; Turkenburg, J. P.; Christiansen, L.; Huge-Jensen, B.; Norskov, L.; Thim, L.; Menge, U. *Nature* **1990**, *343*, 767–770. (b) Winkler, F. K.; D'Arcy, A.; Hunziker, W. *Nature* **1990**, *343*, 771–774.

(3) (a) Dijkstra, B. W.; Drenth, J.; Kalk, K. H. *Nature* **1981**, *289*, 604–606. (b) Dennis, E. A. *Enzymes* **1983**, *16*, 307–353.

(4) (a) Dijkstra, B. W.; Kalk, K. H.; Hol, W. G. J.; Drenth, J. *J. Mol. Biol.* **1981**, *147*, 97–123. (b) Noel, J. P.; Bingman, C. A.; Deng, T.; Dupureur, C. M.; Hamilton, K. J.; Jiang, R.-T.; Kwak, J.-G.; Sekharudu, C.; Sundaralingam, M.; Tsai, M.-D. *Biochemistry* **1991**, *30*, 11801–11811.

(5) (a) Wells, J. A.; Estell, D. A. *TIBS* **1988**, *13*, 291–297. (b) Sprang, S.; Standing, T.; Fletterick, R. J.; Stroud, R. M.; Finer-Moore, J.; Xuong, N.-H.; Hamlin, R.; Rutter, W. J.; Craik, C. S. *Science* **1987**, *237*, 905–909. (c) Craik, C. S.; Roczniak, S.; Largman, C.; Rutter, W. J. *Science* **1987**, *237*, 909–913. (d) Corey, D. R.; McGrath, M. E.; Vásquez, J. R.; Fletterick, R. J.; Craik, C. S. *J. Am. Chem. Soc.* **1992**, *114*, 4905–4907.

0002-7863/93/1515-8523$04.00/0

Table I. Data for Kinetics and Conformational Stability of WT PLA2 and Mutants

	kinetics[a]		conformational stability[b]		
enzymes	$k_{cat,app}$ (s^{-1})	$K_{m,app}$ (mM)	$\Delta G_d^{H_2O}$ (kcal/mol)	$D_{1/2}$ (M)	m (kcal/mol·M)
WT PLA2	675	1.4	9.5	6.9	1.47
H48N	0.04	2.6	6.5 (−3.0)	5.4	1.20
H48Q	undetectable (<0.001)		8.9 (−0.6)	6.6	1.34
H48A	undetectable (<0.001)		6.4 (−3.1)	6.3	1.02

[a] The error limit is estimated to be ±5% for $k_{cat,app}$ and ±15% for $K_{m,app}$ for WT PLA2. [b] The error limit for $\Delta G_d^{H_2O}$ is estimated to be ±0.3 kcal/mol. Numbers in parentheses are differences between mutants and WT, i.e., $\Delta\Delta G_d^{H_2O}$. $D_{1/2}$ is the concentration of Gdn–HCl at the midpoint of unfolding.

that while the δ_1-nitrogen of His-48 is critical to catalysis by PLA2, the ϵ_2-nitrogen of the same residue (which is responsible for the H-bond between Asp and His) plays an important structural role.

Results and Discussion

Kinetic Analysis of Mutants. Three site-specific mutants of PLA2 were constructed by replacing His-48 with Asn, Gln, and Ala; the resulting mutant enzymes are abbreviated as H48N, H48Q, and H48A, respectively. All three mutants presented similar profiles on cation- and anion-exchange columns and were purified to homogeneity as judged by SDS-PAGE analysis with silver staining. The kinetic study of these three mutants was performed with DC_8PC micelles as the substrate and pH state as the method of detection.[4b,7] Table I lists the apparent kinetic constants $k_{cat,app}$ and $K_{m,app}$.[8] For H48Q and H48A mutants, no activity could be detected even at 3 mg of enzyme per assay; the upper limit of the catalytic activity of these two mutants was estimated to be 0.001 s^{-1}. H48N is the only mutant displaying detectable activity, with a $k_{cat,app}$ of 0.04 s^{-1} and a $K_{m,app}$ of 2.6 mM.

As shown in Figure 1 and according to Fersht,[9] the amide nitrogen atoms of Asn and Gln can mimic the δ_1-nitrogen and the ϵ_2-nitrogen, respectively, of His. Since the orientation of the imidazole ring of His-48 in the crystal structure of PLA2[4] is such that the δ_1-nitrogen is H-bonded to the catalytic water molecule and the ϵ_2-nitrogen is H-bonded to Asp-99, the perturbation in catalysis is expected to be greater for H48Q (and H48A) than for H48N. Such a prediction has been supported by the kinetic data shown in Table I.

Although it is tempting and logical to conclude that the kinetic data support the functional role of the δ_1-nitrogen of His-48 as suggested by the crystal structure, we adhered to the dogma of analyzing the structural property before interpreting the kinetic data of the mutants. The structural property was analyzed by two methods: assessment of the global conformational change by 1D and 2D proton NMR and determination of the conformational stability by Gdn–HCl-induced denaturation.[10]

Structural Analysis by Proton NMR. Characterization of the global structural perturbations of the three H-48 mutants was performed using 1D and 2D proton MMR. Figure 2 shows the 1D NMR spectra of all three mutants along with that of WT. The spectra of all three mutants show some perturbation relative to that of WT. The perturbation is particularly extensive for H48N and H48A, which are characterized by dwindling chemical shift dispersion in the aromatic region and broadening throughout the entire spectra. Such a pattern of changes is further manifested in the 2D NOESY spectra shown in Figure 3: the spectrum of H48Q is very similar to that of WT, but those of H48N and H48A have lost most of the NOESY cross-peaks.

The nature of the structural perturbation in H48N and H48A cannot be readily characterized due to the featureless NOESY spectra; however, it is important to point out that the CD spectra showed little change relative to WT, as shown in Figure 4. Thus, the perturbations in these two mutants appear to lie in the tertiary structure and/or the dynamics instead of the secondary structures. On the other hand, the conformation of H48Q can be said to be nearly identical to that of WT: comparison of the chemical shifts of the corresponding resonances between WT and H48Q, derived from NOESY and COSY (not shown) spectra and listed in Table

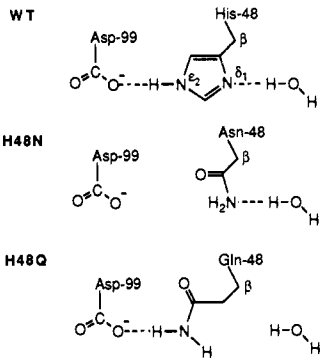

Figure 1. Catalytic diad of PLA2 (top) according to crystal structures[4] and possible orientations of the corresponding residues in the mutants H48N (middle) and H48Q (bottom). Notice that the catalytic diad of PLA2 differs from the catalytic triad of serine proteases in the syn/anti orientation of the carboxylate and the orientation of the imidazole ring.

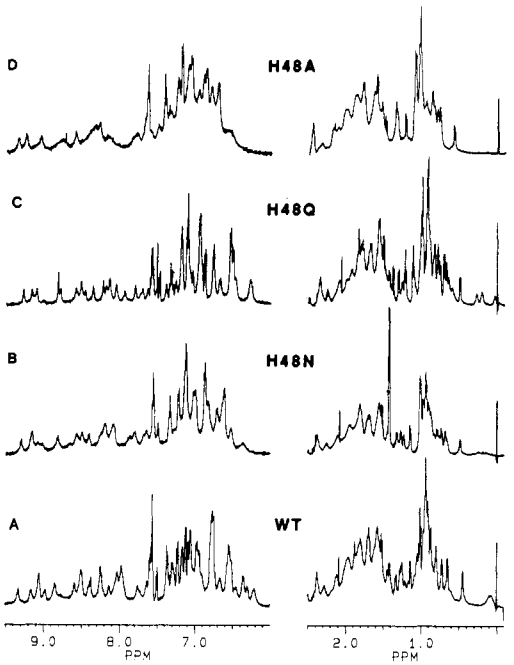

Figure 2. 1D proton NMR spectra of WT (A), H48N (B), H48Q (C), and H48A (D). Sample conditions are described in the Experimental Section. The FID were processed with Gaussian multiplication (LB = −5, GB = 0.1) prior to Fourier transformation. The relative signal intensities between aliphatic and aromatic regions of each spectrum were not on the same scale.

(6) Deng, T.; Noel, J. P.; Tsai, M.-D. *Gene* **1990**, *93*, 229–234.
(7) (a) Dupureur, C. M.; Yu, B.-Z.; Jain, M. K.; Noel, J. P.; Deng, T.; Li, Y.; Byeon, I.-J. L.; Tsai, M.-D. *Biochemistry* **1992**, *31*, 6402–6413. (b) Dupureur, C. M.; Yu, B.-Z.; Mamone, J. A.; Jain, M. K.; Tsai, M.-D. *Ibid.* **1992**, *31*, 10576–10583.
(8) The kinetic parameters $k_{cat,app}$ and $K_{m,app}$ are considered as apparent since the assays using micelles do not separate the steps of E to E* (enzyme bound to the interface) and E* to E*S (enzyme-substrate complex at the interface). According to our recent studies,[7] however, the relative $k_{cat,app}$ values of DC_8PC micelles accurately reflect the relative k_{cat} values in the scooting mode assay system[12] for a series of PLA2 mutants. This is even more likely to be the case for the H48 mutants for which the chemical step will definitely be rate-limiting. Due to the low activity of these mutants, the scooting mode analysis was not performed.
(9) Leatherbarrow, R. J.; Fersht, A. R. *Biochemistry* **1987**, *26*, 8524–8528.
(10) Pace, C. N. *Methods Enzymol.* **1986**, *131*, 266–279.

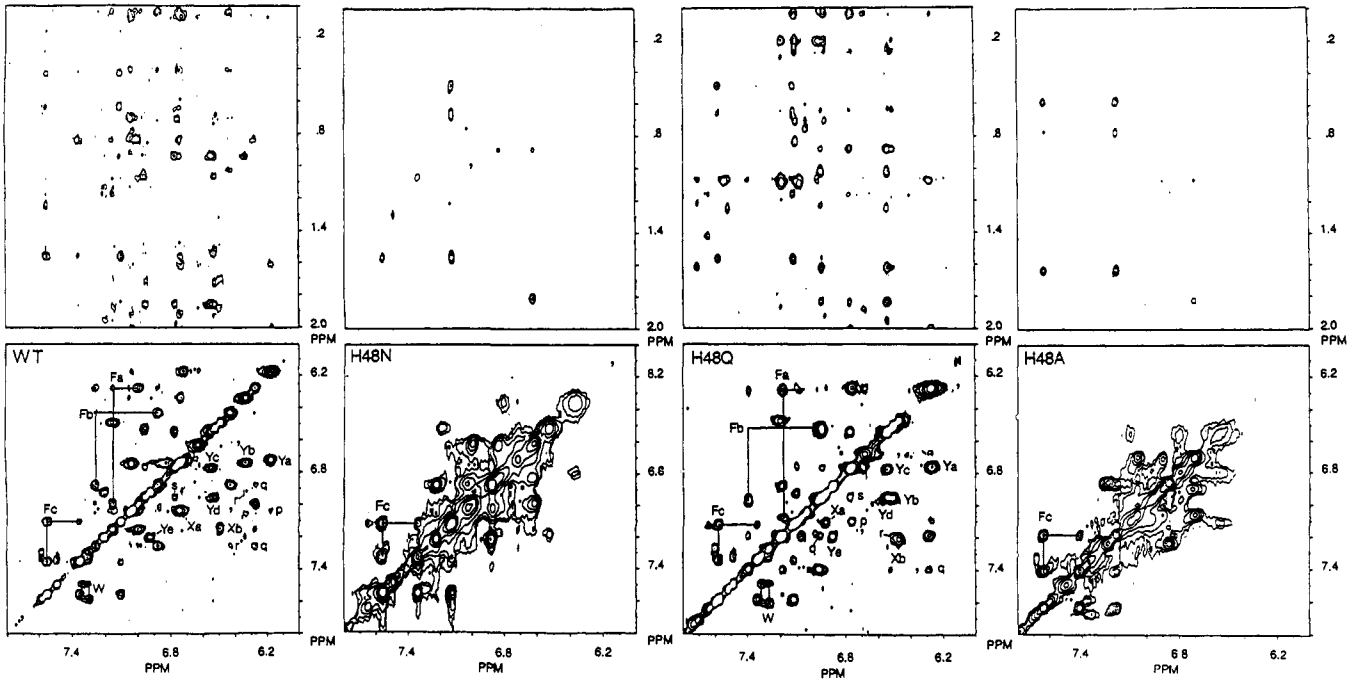

Figure 3. Phase-sensitive NOESY spectra (showing the aromatic–aromatic and aromatic–aliphatic regions) of WT, H48N, H48Q, and H48A in D_2O at 37 °C, 500 MHz. Sample conditions, data acquisition, and data processing parameters are described in the Experimental Section. The aromatic spin systems (F, Y, and W, designating Phe, Tyr, and Trp, respectively) and the interresidue NOESY cross-peaks (small letters p–s) have been described previously.[7,13]

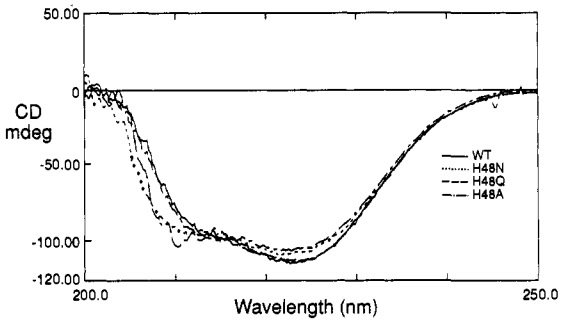

Figure 4. CD spectra of WT, H48N, H48Q, and H48A in the native form. Sample conditions are described in the Experimental Section.

Table II. Proton Chemical Shifts of the Assigned Residues of WT PLA2 and the H48Q Mutant[a]

spin system[b]	possible assignmts[c]	WT			H48Q		
Fa	(F5)	6.28	7.00	7.15	6.28	7.08	7.19
Fb	F106	*6.43*	6.88	*7.26*	*6.57*	6.96	*7.40*
Fc	F94	7.10	7.35	7.55	7.12	7.34	7.58
Ya	Y111	6.18	6.72		6.28	6.76	
Yb	Y52	*6.34*	*6.74*		*6.51*	*6.95*	
Yc	Y73	6.55	6.78		6.54	6.78	
Yd	Y75	6.52	6.95		6.55	6.95	
Ye	Y69	6.92	7.20		6.88	7.19	
W	W3	7.30	7.34	7.48	7.27	7.32	7.48
		7.58			7.60		
Xa	(F22)	*6.75*	7.04		*6.92*	7.11	
Xb	(Y28)	6.49	7.15		6.47	7.21	
L1	(L41)	0.07			0.04		
L2	L58	0.63	0.44		0.66	0.49	
IG	I95	0.94			0.88		
A1	(A55)	1.56			1.57		
M	(M8)	1.86			1.84		

[a] The italicized numbers are resonances which differ by >0.10 ppm between WT and H48Q. [b] The designation of spin systems is based on previous work in this and other laboratories.[7,13] [c] Parentheses indicate tentative assignments.

II, indicates that only 5 out of the 33 identified resonances differ by greater than 0.1 ppm. The most notable difference is a mere 0.2 ppm shift in Y52, whose aromatic ring is located in the immediate vicinity of the imidazole ring of His-48.

Conformational Stability. The conformational stability of the mutants was determined by Gdn–HCl-induced denaturation assuming a two-state folding mechanism, according to the standard equation

$$\Delta G_d = \Delta G_d^{H_2O} - m(\text{Gdn–HCl})^{10} \quad (1)$$

where ΔG_d is the Gibbs free energy of denaturation at various concentrations of Gdn–HCl, $\Delta G_d^{H_2O}$ is that extrapolated to zero concentration of Gdn–HCl, and m is a constant related to the susceptibility of the enzyme toward denaturation by the denaturant. The results of this Gdn–HCl-induced denaturation study are also listed in Table I. In support of the NMR results, the free energy of denaturation $\Delta G_d^{H_2O}$ is very similar between WT and H48Q but decreases by 3 kcal/mol for both H48N and H48A.

Structural Role of His-48. The results of both NMR and conformational stability analyses strongly suggest that the Asp-99···His-48 hydrogen bond, which can be retained in H48Q but not in H48N or H48A, is important in maintaining the conformational integrity of PLA2. Although it can be argued that any H-bond within a protein is likely to contribute to structure, the observation described in this work is unique in its magnitude and in the fact that the role of this H-bond in serine proteases is thought mainly to orient the His in the proper conformation and the correct tautomeric form.[5b-d]

Overall, the structural properties of H48N and H48A have some resemblance to that of D99N (Asp-99 to Asn mutant) reported previously,[11] which was interpreted as being highly flexible in conformation. The previous study, however, did not allow us to pinpoint the importance of the Asp-99···His-48 hydrogen bond since the carboxylate group of Asp-99 is involved in four H-bonds with surrounding groups according to the crystal structure.[4] The results of this work and the previous paper[11] taken together suggest that the entire catalytic diad plays an important structural role.

(11) Dupureur, C. M.; Li, Y.; Tsai, M.-D. *J. Am. Chem. Soc.* **1992**, *114*, 2748–2749.

Functional Role of His-48. Since the structure of H48Q is largely unperturbed relative to that of WT, the change in kinetics can be attributed to the catalytic role of the δ_1-nitrogen of His-48. The activity of this mutant was undetectable, but an estimation of >8 kcal/mol can be obtained on the basis of the upper limit of activity. The result not only supports the prediction on the basis of the X-ray structure as shown in Figure 1 but also provides an estimation of the energetics of the contribution to catalysis by the δ_1-nitrogen of His-48.

Since H48N retains the δ_1-nitrogen as shown in Figure 1, it is expected to display higher catalytic activity relative to H48Q. This prediction has been supported by the kinetic data in Table I. However, the kinetic data of H48N cannot be used to determine the energetic contribution of the ϵ_2-nitrogen of His-48 to catalysis. The decreased activity in this mutant is caused by not only the removal of the Asp-99···His-48 hydrogen bond but also the resulting global structural perturbation. Interestingly, the activity is still detectable despite the odds.

Conclusion. Although the amide nitrogens of Asn and Gln are not structurally perfect mimics of the δ_1-nitrogen and the ϵ_2-nitrogen, respectively, of His, we have been able to use this approach to demonstrate that the two nitrogens of His-48 serve two important but different functions. Our conclusion of the important structural role played by the catalytic diad also suggests that the structure–function relationship of enzymes is more complicated than currently realized.

Experimental Section

Materials and General Methods. Oligonucleotides were purchased from Bio-Synthesis (Lewisville, TX) and used without further purification. Mutagenesis and sequencing kits were purchased from Amersham and United States Biochemicals, respectively. DC_8PC was obtained from Avant Polar Lipids (Birmingham, AL). Ultrapure Gdn–HCl was purchased from ICN Biochemical. 99.9 atom % D D_2O, "100%" D D_2O, and TMSP-d_4 were obtained from MSD Isotopes. DCl was purchased from Cambridge Isotopes. The Fast Flow Sepharose-S and -Q resins (cation and anion exchangers, respectively) were obtained from Pharmacia–LKB. Other chemicals and biochemicals were of the highest quality available commercially. FPLC experiments were performed on a Pharmacia-LKB FPLC system. SDS-PAGE analyses of proteins were performed with the Phast System (Pharmacia LKB) on 20% acrylamide gels.

Site-Directed Mutagenesis and Protein Purification. Site-directed mutants were generated with oligonucleotides 5′GCAATTATCATTTGTTTGGCA3′ (His-48 to Asn), 5′GCAATTATCCTGTGTTTGGCA3′ (His-48 to Gln), and 5′GCAATTATCAGCTGTTTGGCA3′ (His-48 to Ala) by using a mutagenesis kit according to the manual provided by the manufacturer. Since the mutation efficiency was very high, the mutants were selected by DNA sequencing according to Sanger's dideoxy method using a DNA sequencing kit. The recombinant PLA2 and mutants were isolated from the *E. coli* expression host BL21(DE3)[plysS] carrying the pTO–PLA2 plasmid (H. Zhu, unpublished results) which was a modification of the pTO–proPLA2 plasmid constructed previously.[6] The enzymes thus obtained were in the mature form without the prosequence. The procedure for purification was similar to those described for the recombinant PLA2 carrying the prosequence,[4b,7] except for the omission of the activation step.

Kinetic Measurements. Activities of the enzyme toward micellar substrate DC_8PC were measured at 45 °C with a Radiometer RTSS Titration System as previously described.[4b] The final reaction solution for kinetic analysis contained 1 mM borate, 25 mM $CaCl_2$, 100 mM NaCl, 0.1 mM EDTA, and 1–5 mM DC_8PC at pH 8.0. The apparent V_{max} and K_m were determined using Eadie–Hofstee plots[14] of v vs $v/[S]$. On the basis of the PLA2 molecular weight of 13 500 Da, the apparent k_{cat} was calculated from V_{max}.

NMR Methods. All proton NMR experiments were conducted in D_2O at 37 °C and pH 4.0–4.1 (uncorrected pH from pH meter reading) on a Bruker AM-500 spectrometer. Typical NMR sample preparation is described as follows. The enzyme sample was dissolved in D_2O (99.9 atom % D) and mixed with stock solutions of $CaCl_2$ and NaCl, both in D_2O. The pH of the solution was adjusted to 4.1–4.3 (uncorrected) with DCl and NaOD stock solutions. The solution was then kept at room temperature for 8 h to allow for deuterium exchange and was lyophilized and the procedure repeated. The lyophilized sample was dissolved in 0.5 mL of "100%" D_2O, and the pH was adjusted to 4.0–4.1 (uncorrected) with the same DCl and NaOD stock solutions. The final NMR samples contained 1.5–2.0 mM enzyme, 50 mM $CaCl_2$, and 200 mM NaCl (300 mM NaCl for WT). TMSP was used as an internal chemical shift reference.

Standard pulse sequences and phase cycling were used for 2D NMR experiments: DQF-COSY[15] and NOESY.[16] The mixing time for NOESY experiments was 200 ms. All spectra were obtained in the phase-sensitive mode with quadrature detection in the $f1$ dimension by time-proportional incrementation.[17] A 4096 × 512 matrix in time domain was recorded and zero-filled to a 4096 × 2048 matrix prior to multiplication by an unshifted sine bell function (SSB1 = SSB2 = 0) for COSY and by a Gaussian function (LB2 = −3, GB2 = 0.1) in the $f1$ dimension and a shifted sine bell function (SSB1 = 12) in the $f2$ dimension for NOESY.

CD Spectroscopy and $\Delta G_d^{H_2O}$ Measurements. CD spectra were recorded on a JASCO J-500C spectropolarimeter, and the data were processed with DP-500/AT system (version 1.29) software. Stock solutions of 5 mM enzyme and 8.6 M Gdn–HCl were prepared in a buffer containing 10 mM borate and 0.1 mM EDTA at pH 8.0. The precise concentrations of the enzyme and Gdn–HCl were determined spectrophotometrically and by the refractive index method,[18] respectively. Typical CD samples contained, in the borate buffer mentioned above, 0.08 mg of the enzyme and Gdn–HCl in concentrations varying from 0 to 8.5 M. Calcium ions were not included since in the presence of Ca^{2+}, the WT PLA2 was so stable that the entire denaturation curve could not be obtained with Gdn–HCl. The spectra were recorded at 30 °C with a spectral width from 200 to 250 nm and with 5 scans. After the corresponding background was subtracted, the ellipticity at 222 nm of each CD sample was recorded and used to calculate the Gibbs free energy of unfolding.

Acknowledgment. We thank H. Zhu for initial technical assistance in mutagenesis experiments and Y. Ji for purifying some of the H48N mutant. This work was supported by Research Grant GM41788 from NIH. The Bruker AM-500 NMR spectrometer at The Ohio State University used for this study was partially funded by NIH Grant RR 01458.

(12) Jain, M. K.; Gelb, M. H. *Methods Enzymol.* **1991**, *197*, 112–125.
(13) Fisher, J.; Primrose, W. U.; Roberts, G. C. K.; Dekker, N.; Boelens, R.; Kaptein, R.; Slotboom, A. J. *Biochemistry* **1989**, *28*, 5939–5946.
(14) Atkins, G. L.; Nimmo, I. A. *Biochem. J.* **1975**, *149*, 775–777.
(15) Rance, M.; Sørensen, O. W.; Bodenhausen, G.; Wagner, G.; Ernst, R. R.; Wüthrich, K. *Biochem. Biophys. Res. Commun.* **1983**, *117*, 479–485.
(16) Bodenhausen, G.; Kogler, H.; Ernst, R. R. *J. Magn. Reson.* **1984**, *58*, 370–388.
(17) Marion, D.; Wüthrich, K. *Biochem. Biophys. Res. Commun.* **1983**, *113*, 967–974.
(18) Nozaki, Y. *Methods Enzymol.* **1972**, *26*, 43–50.